

PAPER

## Blast Load Assessment: RC Wall Subjected to Blast Load

To cite this article: M A Seman *et al* 2019 *IOP Conf. Ser.: Earth Environ. Sci.* **244** 012007

View the [article online](#) for updates and enhancements.



**IOP | ebooks™**

Bringing you innovative digital publishing with leading voices to create your essential collection of books in STEM research.

Start exploring the collection - download the first chapter of every title for free.

# Blast Load Assessment: RC Wall Subjected to Blast Load

M A Seman<sup>1</sup>, S M Syed Mohsin<sup>1</sup> and Z M Jaini<sup>2</sup>

<sup>1</sup>Faculty of Civil Engineering & Earth Resources, Universiti Malaysia Pahang

<sup>2</sup>Faculty of Civil & Environmental Engineering, Universiti Tun Hussein Onn Malaysia

mazlan@hotmail.co.uk

**Abstract.** The evaluation of the pressure produced by blast load on the structure surface and selected location around with the aid of hydrocodes is studied in this paper. The existing knowledge of predicted blast pressure has been embraced in this paper for initial design in engineering application. The acquired blast parameters from numerical results are compared with blast test data and empirical methods. Besides the comparison, the effects of mesh distribution and air volume size on pressure are also studied. The numerical simulation initially conducted in 3D free air explosion and followed by the consideration of an obstruction structure on the blastwave propagation. The numerical peak incident overpressure indicated, the pressure of 0.51 MPa at 4.62 msec is approximates the overpressure recorded in the explosive test carried out at Fort Leonard Wood Army Base. It is revealed numerically, the overpressure at the bottom part on the wall surface experienced the higher overpressure.

## 1. Introduction

Aggressors attack using improvised explosive not the only source for the blast load. Some commercial equipment and human daily activities can contribute as well, such as electrical transformer, gas pipelines and industrial plants during the operation. The explosion generates overpressure, which may injure people and damage any object on its path. Generally, the pressure propagates radially in all direction from the explosion centre at supersonic speed. Prior studies regarding the blast pressure on object had been conducted over the past half century [1-6]. Basically, the recommended expression is based on standoff distance and charge weight as an equivalent mass of Trinitrotoluene (TNT) to predict the blast peak overpressure. The reflected overpressure resulted from the reflection wave due to obstacle also been modelled [6]. Besides the empirical expressions, the Unified Facilities Criteria (UFC) manuals are widely used for blast pressure parameters. The manuals contain data on explosive tests using charge weight from less than 1kg up to 400,000kg [7-8]. Nowadays, the predictions of blast pressure-time history in related engineering problems are viable in line with the rapid development of computer technology and the advancement of numerical techniques [9]. In this paper, the empirical and numerical methods are used to appraise the overpressure parameter for the same charge weight and specific distance. Although there is no available experiment data at required location, the comparison of available data and the projected data at required distances area appraised for both methods in the following section A blast wave originating from closed or free explosion detonation behaves, when interacting with structures, as a short duration dynamic load. Previous studies showed that load with short duration and high magnitude influence significantly the response of the structure and can modify substantially the expected material behaviour. Therefore, the aim of this paper is to



appraise the blast parameters on the structure using empirical and numerical approaches. Then the results from empirical and numerical methods are compared with experimental blast test.

## 2. Blast pressure profile

The blast pressure profile for varies and different sources of origin which are categorised as high explosive (HE) such as conventional bomb and vehicle bomb having typical shape as shown in Figure 1. Before the shock front reaches the given point, the ambient pressure is  $p_o$ . At arrival time  $t_a$ , the pressure rises discontinuously to the peak value of  $p_o + P_s^+$ . The quantity  $P_s^+$  is called as the peak overpressure. The pressure then decays to ambient in a total time of  $t_a + T^+$ , and then drops to a partial vacuum of value  $p_o - P_s^-$ , and eventually returns to the ambient pressure  $p_o$ , in a total time of  $t_a + T^+ + T^-$ . The pressure-time history of the blast wave uses exponential functions as shown in the Friedlander equation as follows; [6].

$$p(t) = p_o + P_s^+ \left(1 - \frac{t - t_a}{T^+}\right) e^{-b(t - t_a)} \quad (1)$$

Where  $t$  is time,  $p_o$  is the ambient pressure,  $p_s$  is the peak overpressure,  $T_s$  is the duration of the positive phase,  $t_a$  is the arrival time and  $b$  is a positive constant of waveform parameter that depending on the peak overpressure. The two most influential parameters of the blast environment, including the charge weight  $W$ , and the standoff distance ( $R$ ) between the blast source and the target. In practice, the charge weight ( $W$ ) is identified as an equivalent mass of TNT in kilograms. Therefore, for any distance ( $R$ ) from an explosive charge ( $W$ ) can be transformed into a characteristic scaled distance ( $Z$ ) which is known as scaling laws. The scaling law provides parametric correlations between a particular explosion and a standard charge of the same substance [10].

$$Z = R \left( \frac{W}{\text{TNT}} \right)^{-1/3} \quad (2)$$

According to Department of Defence, USA [8], based on the confinement environment around the explosive, blast loads can be categorised into two main types comprising unconfined and confined explosion. The main type can be subcategorised based on blast load producing within the structure or acting on the structures. For unconfined explosions, the blast loading can be subcategorised into free-air explosion, air explosion and surface explosion. While for the confined explosions, it can be fully vented, partially confined and fully confined. According to the present study, unconfined explosion is related and discussed. When an explosion occurs without obstructions in the air medium to amplify the radially propagating blast wave between the explosive charge and structure, the blast load on the structure is free-air explosion. The distance above the ground to the explosive centre usually is about two to three times the height of structure [8]. An air explosion produces by the explosive above the ground and at distance away from the structure, the initial blast wave, propagating away, impinges on the ground surface prior arrival at the structure. If the explosive charge is located above the ground at the height of burst (HOB) within 1-2 meter, the blast is considered as a surface explosion. The initial incident blast waves of the explosion are reflected and amplify by the ground surface to produce a reflected blast wave. Therefore, the blast wave front forms a hemispherical blast wave that propagates toward the target. Surface explosion is different from an air explosion, where the incident and reflected blast wave merge instantly [11-12].

A correlation between surface (hemispherical) explosion and free-air (spherical) explosion implies that if the ground surface is a perfect reflecting surface, the explosive charge weight for surface explosion would be effectively double. However, due to the energy dissipated in producing a ground crater and ground shock, a conversion unit approximately 1.7-1.8 needs to consider. [12-13]. When an explosion occurs with an obstruction to the propagating blast wave such as wall structure, as the blast wave strike the wall surface at a normal angle of incidence ( $\alpha$ ), the incident overpressure is magnified because the blast wave propagation moving through the air suddenly has arrested and redirecting by the wall surface. As a result, the reflected overpressure ( $P_r$ ) becomes 2-8 times higher than normal as

reported by ASCE [14], while Uddin [12] reported that the reflected overpressure could increase up to 13 times. The highest values could rise up to 20 times more than the incident overpressure [15-16]. The angle of incidence ( $\alpha$ ) on a surface is the angle between the outward normal and the direct vector from explosive charge to the point as illustrated in Figure 2. For the given scaled distance and angle of incidence is zero ( $\alpha=0$ ), it is fully reflected overpressure. Equation (3) indicates the effective distance ( $R_e$ ) based on angle of incident. The peak incident overpressure remains close to its fully reflected value if the angle of the incident less than 45 degree according to Remmenikov [11] and also can be estimated by analysing the reflected pressure-angle of incidence relationship curve in UFC 3-340-2 [8].

$$R_e = (R^2 + h^2)^{1/2} \quad (3)$$

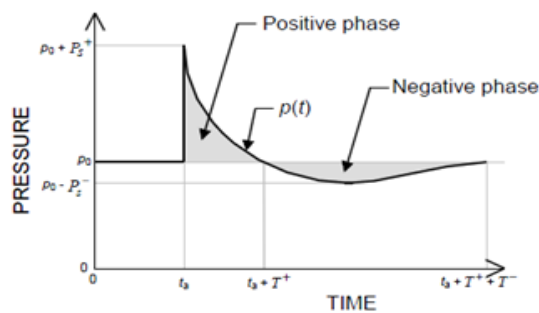


**Figure 1.** Pressure-time history of an ideal blast pressure

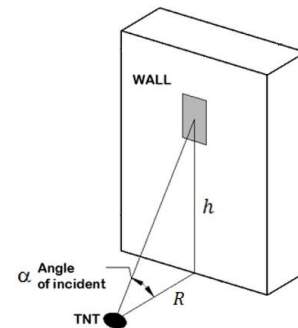


**Figure 2.** Angle of incident and actual effective distance

### 3. Prediction of blast pressure

There are many suggested solutions for the prediction of blast wave parameters studies. The main approaches can be divided into three methods: (1) analytical or empirical methods using correlations with experimental data, which most of the approaches are limited to underlying experimental database; (2) semi empirical methods based on simplified model of physic phenomena. These methods, which rely on extensive data and case study,; (3) numerical analysis based on mathematical equations that describe the basic law of physic including conversion of mass, momentum and energy.

#### 3.1. Empirical

The following empirical equations for the shock wave parameter are based on scaled distance. Brode [1] introduced the estimation of peak incident overpressure due to spherical explosion follows;

$$P_{so} = \frac{6.7}{Z^3} + 1 \text{ for } P_{so} > 10 \text{ (in bar)} \quad (4)$$

$$P_{so} = \frac{0.975}{Z} + \frac{1.455}{Z^2} + \frac{5.850}{Z^3} - 0.019 \text{ for } 0.1 < P_{so} < 10 \text{ (in bar)} \quad (5)$$

Newmark and Hansen [2] introduced a relationship in calculating the incident overpressure for ground surface explosion as follows:

$$P_{so} = 6784 \frac{W}{R^3} + 93 \left( \frac{W}{R^3} \right)^{1/2} \text{ (in bar)} \quad (6)$$

Henrych [3] introduced peak overpressure according to range of scaled distance  $Z$  as follows;

$$P_{so} = \frac{1.4072}{Z} + \frac{0.5540}{Z^2} - \frac{0.0357}{Z^3} + \frac{0.000625}{Z^4} \text{ if } 0.05 \leq Z \leq 0.3 \text{ (in MPa)} \quad (7)$$

$$P_{so} = \frac{0.6194}{Z} - \frac{0.0326}{Z^2} + \frac{0.2132}{Z^3} \text{ (MPa) if } 0.4 \leq Z \leq 1.0 \text{ (in MPa)} \quad (8)$$

$$P_{so} = \frac{0.0662}{Z} + \frac{0.4050}{Z^2} + \frac{0.3288}{Z^3} \text{ (MPa) if } 1.0 \leq Z \leq 10 \text{ (in MPa)} \quad (9)$$

Mill [5] introduced peak incident overpressure as follows;

$$P_{so} = \frac{1772}{Z^3} + \frac{114}{Z^2} + \frac{108}{Z} \text{ (in kPa)} \quad (10)$$

When the propagating blast wave encounters an obstacle perpendicular to its direction, the reflection wave increases the incident overpressure to a maximum reflected overpressure ( $P_r$ ) as in Equation (11) where  $P_o$  is ambient pressure [13] as follows;

$$P_r = 2P_{so} \left( \frac{7P_o + 4P_{so}}{7P_o + P_{so}} \right) \quad (11)$$

Other than empirical equations, the manuals of Unified Facilities Criteria (UFC) based on Department of Defense, USA are also used widely as the empirical method. The UFC 3-340-2 [8] manual supersedes TM 5-1300 manual using in both military and civilian sectors for designing structures which provide protection against the blast effect of accidental explosion. From the manual, the design curves show the blast pressure parameters in the function of scaled distance  $Z$  for all unconfined explosions such as peak overpressure ( $P_{so}$ ), peak reflected overpressure ( $P_r$ ) and time of arrival ( $t_a$ ). Besides UFC 3-340-2, UFC 3-340-1 [7] superseded TM 5-855-1, it was intended for designing hardened facilities to resist the effect of conventional weapons. This includes criteria for protection against penetrating weapons, contact detonation, and blast and fragmentation from a standoff distance. However, this manual is restricted document and for official use only.

Kingery and Bulmash [4] developed the equation in predicting blast parameters from spherical air explosion and hemispherical surface explosion. The equations have been automated in computer program known as ConWep. ConWep is a collection of conventional weapons effect calculating from the equation and curves of UFC 3-340-1. Unlike UFC 3-340-1, where the approximation equivalent triangular pulse is proposed to present the decay of overpressure and reflected overpressure, ConWep uses a realistic approach in assuming an exponential decay of the pressure with time as follows;

$$P_t = P_{so} \left( 1 - \frac{t-t_a}{t_o} \right) \exp \left( \frac{b(t-t_a)}{t_o} \right) \quad (12)$$

Where  $P(t)$  is the pressure at time  $t$  (kPa);  $P_{so}$  is the peak incident pressure (kPa);  $t_o$  is the positive phase duration (msec);  $b$  is the decay coefficient (dimensionless); and  $t_a$  is the arrival time (msec). The equation 12 is usually referred to as the Friedlander equation. This equation is widely accepted as engineering predictions for determining free-field pressures and loads on structures. The correlations between decay coefficient  $b$  and scaled distance  $Z$  are used same as [17];

$$b = Z^2 - 3.7Z + 4.2 \quad (13)$$

### 3.2. A subsection

Numerical simulation is one of the methods to replace an expensive blast test currently. The AUTODYN [9] simulation package is used in the present study. AUTODYN is an integrated explicit analysis tool program especially for modelling non-linear dynamic problems using finite element, finite volume and mesh-free particle to solve nonlinear dynamic problems of solid, fluids, gas and their interactions. Besides an integrated explicit analysis tool program, AUTODYN also offers multi-

solver coupling for multi-physic including coupling between Finite Element (FE), Computational Fluid Dynamic (CFD) and Smoothed Particle Hydrodynamics (SPH).

The Arbitrary Lagrange Euler (ALE) is the numerical approach for the interface analysis between air and structure. This approach allows different part of the solvers such as structure, fluids and gases, these can be modeled simultaneously using Lagrange and Euler approaches. These different solvers are then coupled together in space and time. In the numerical model, air is modelled by an ideal gas EOS, which is one of the simplest forms of EOS. The pressure is related to enery that can be written as follows:

$$p = (\lambda - 1) \rho e \quad (14)$$

where  $\gamma$  is a ratio of specific heat and  $\rho$  is air density.  $e$  is the specific internal energy, with the gamma law EOS under standard atmosphere pressure and  $\gamma=1.4$ , its initial energy is  $e=2.068 \times 10^5$  kJ/kg. In the simulation, the standard constants of air from the AUTODYN material library [9] are used. TNT the high explosives are typically modeled using the Jones-Wilkins-Lee (JWL) EOS, which model the pressure is generated by chemical energy and can be represent as follows:

$$P = A \left( 1 - \frac{\omega}{R_1 V} \right) e^{-R_1 V} + B \left( 1 - \frac{\omega}{R_2 V} \right) e^{-R_2 V} + \frac{\omega E}{V} \quad (15)$$

where P is the detonation of high explosive; V is the specific volume; E is specific internal energy; and A, B,  $R_1$ ,  $R_2$  and  $\omega$  are material constant. In the present simulation, for the TNT explosive charge, A, B,  $R_1$ ,  $R_2$  and  $\omega$  are  $3.7377 \times 10^5$  MPa,  $3.747 \times 10^3$  MPa, 4.15, 0.9 and 0.35, respectively.

#### 4. Structure subjected to blast load

In the present study, the experimental result of the reinforced concrete (RC) wall structure subjected to blast load [18] was appraised based on the blast pressure parameter. The reinforced concrete wall was reinforced with 16 mm diameter on vertical reinforcement and 10 mm diameter on transverse stirrups, both at 152 mm spacing. The concrete cover on all sides of the walls is 25 mm thick. The cylinder compressive strength of the concrete is 44 MPa with standard deviation of 1.38 MPa; the Modulus of Elasticity is 31.5 GPa with a standard deviation of 827 MPa. The reinforcement has yield strength of 619 MPa and Young's modulus of 200 GPa. Figure 3 shows the geometry and section detail of the wall. The walls have a cross-sectional dimension of 1829 mm  $\times$  1219 mm with wall thickness of 152 mm and 305 mm thickness of footing. According to the study, the wall was tested with 4 lbs., 10 lbs. and 30 lbs. TNT charge weight with 4 ft. standoff distance from the centre of the wall. The pressure transducers were placed 18 ft. away from the centre of the charge weight. The blast test was conducted, the result can be revealed, only after the third test with 30 lbs. TNT charge weight, the visible cracks were clearly observed on the front and the back of the wall. The recorded peak overpressure was 0.49 MPa at 4.64 msec. Therefore, in the present study, the highest charge weight and overpressure parameters are considered in the following appraisal.

#### 5. Blast pressure analysis

##### 5.1. Empirical

According to the explosive located in the experimental [18], the blast is categorised as surface explosion. Therefore, the blast pressure parameter for hemispherical explosion in UFC 3-340-2 is used for the analysis. Angle of incident ( $\alpha$ ) and actual effective distance ( $R_e$ ) are considered for the blast pressure mapping on the wall surface. Figure 4 shows, the incident overpressure ( $P_{so}$ ) and reflected overpressure ( $P_r$ ) at the point of interest on the wall surface with 1-degree increment for angle of incident ( $\alpha$ ) until the top edge of the wall. As can be seen, overpressure parameters for Mill's equation is about 2-4 times higher compared to the overpressure parameter for UFC 3-340-2 and Henrych's equation respectively. Since (besides) the UFC 3-340-2 parameters are in between both the empirical equations and also as mentioned by Remennikov [11], all the empirical equations accuracy diminishes

as the explosive event becomes as a near field. Therefore, overpressure parameters from UFC 3-340-2 are considered in the following appraisal.

Figure 5(a) below shows the blast overpressure distribution based on time arrival. As can be seen, it is divided into 11 regions namely as A to K respectively. Figure 5(b) shows the selected incident and reflected overpressure time-history for A, D, G, I and K. It is found that both incident and reflected overpressure are identical in positive duration time and time to reach peak overpressure, but reflected overpressure is higher than incident overpressure with 37.94 MPa at 0.36msec and 4.70 MPa at 0.36 msec respectively for the highest overpressure. Based on ConWep analysis reporting in the report [19] and literature [18], the pressure distribution on the wall surface and pressure-time history at the centre of the wall is highest overpressure recorded with 28.96 MPa at 0.39 msec.

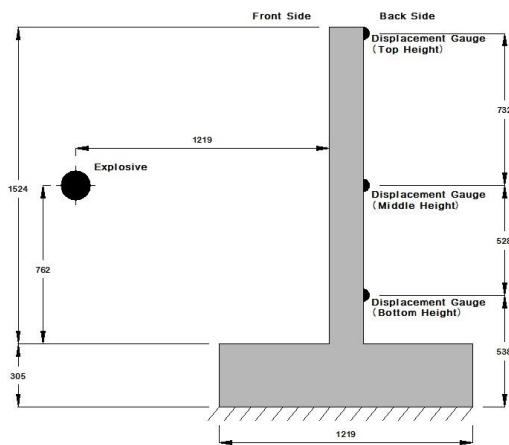


**Figure 3.** Geometry of reinforced concrete wall (unit in mm)

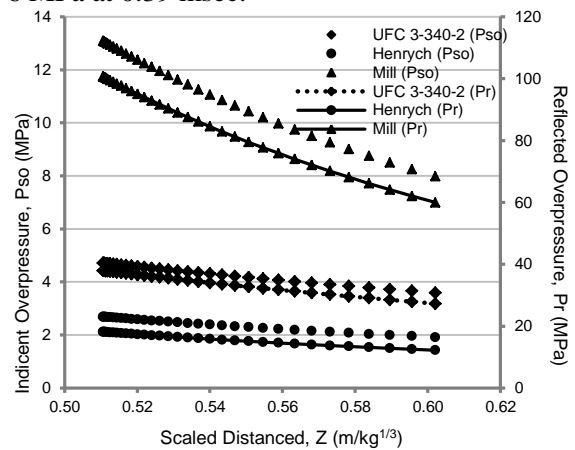


**Figure 4.** Comparison of the peak incident ( $P_{so}$ ) and reflected overpressure ( $P_r$ )

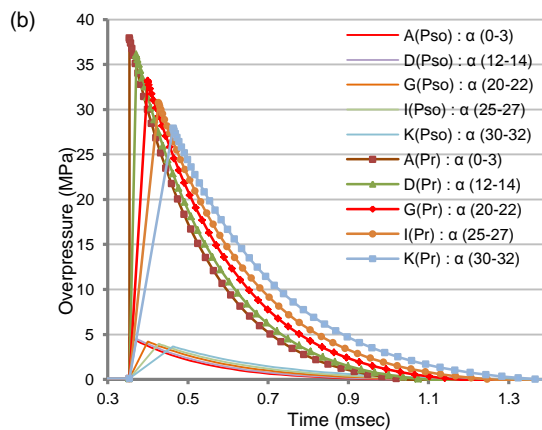
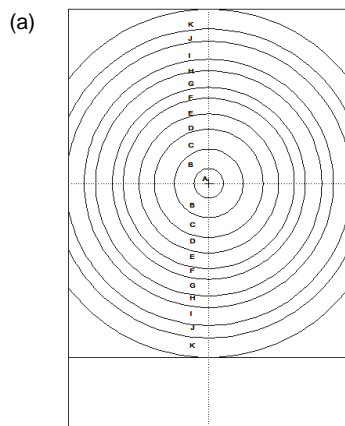


**Figure 5.** Overpressure on the wall surface with UFC 3-340-2 analysis (a)Overpressure distribution. (b)Overpressure-time history

5.2. Numerical

In order to study the free propagation of the blast waves in the air, a 1 m x 1m x 5.5 m air volume was numerically simulated for 30 lbs. TNT charge weight as shown in Figure 6. The wedge consists of blast pressure history is remap in AUTODYN, as it is used to apply the effect 3D explosion. Gauge 1 and 2 are located at 4 ft. and 18 ft. respectively away from centre of the charge weight. Flow out of air is allowed in all the model borders. The simulation was set up for 25 msec, it is that found for Gauge 1 the peak incident overpressure is 2.40 MPa at 1.43 msec, while for Gauge 2 is 0.51 MPa at 4.62 msec

as shown in Figure 7. From the blast test conducted [18], the peak incident overpressure pressure at 18 ft. away from centre of explosive recorded is 0.49MPa at 4.64msec. Therefore, the numerical results on peak incident overpressure for free field agree well with the experimental conducted.

The same wedge using for remap function above is considered in the numerical simulation for an actual blast test. Figure 8 shows the location of the gauges in 2.5 m x 2.0 m x 7 m volume of air with the consideration of reinforced concrete wall in the simulation and assigned outflow boundaries. Gauges 1, 4 and 5 are placed on the wall, which are 4 ft. away from the centre of charge weight. It is placed at the height of 538 mm, 1270 mm and 1798 mm respectively from the ground level. Accordingly, for the same height from the ground level, Gauge 6, 8 and 9 are placed perpendicular from Gauge 1, 4 and 5 respectively on the free side, 4 ft. away from charge weight. Gauge 2 is placed at 18 ft. away and perpendicular to the centre of charge weight. It is found that the simulated data for Gauge 3 is 0.38 MPa at 4.9 msec and the positive duration is 25 msec. Type 3 model for an actual blast test as shown in Figure 9 is considered due to positive duration. The duration for Type 2 air volume is longer than the duration for Type 1 air volume. The air volume is considered on the left and right of the structure in symmetrical geometry.

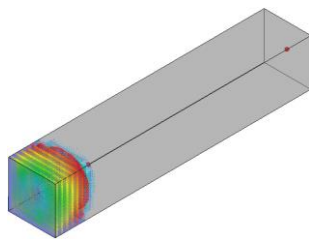


**Figure 6.** Blast simulation in free field (Type 1)

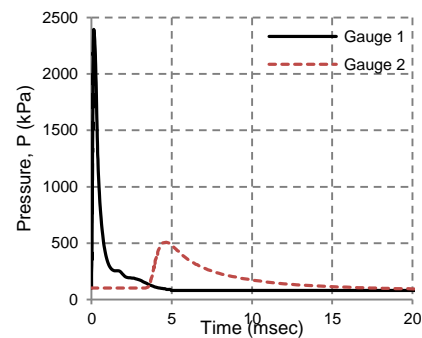


**Figure 7.** Blast overpressure-time history

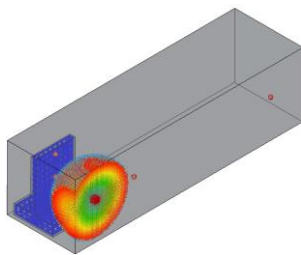


**Figure 8.** Model of blast test (Type 2)

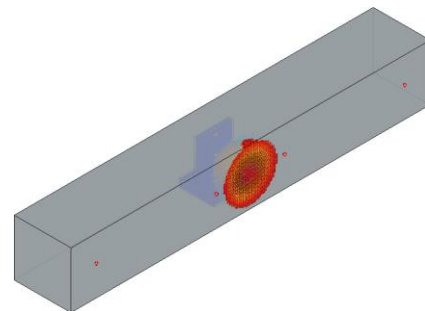


**Figure 9.** Model of blast test (Type 3)

## 6. Comparison on overpressure paremeters

From the results of approximately 32,000 nodes in Autodyn, it can be concluded that proper grid size and arrangement on I,J,K directions of the air volume play important roles in predicting overpressure parameters. Table 1 shows, grid arrangement and overpressure at the location of 18 ft. away. According to the overpressure calculated with A.T Blast software and measured in the literature [18], the simulated data with I,J,K (18,22,72) is selected for further analysis. A great discrepancy exists in the positive time history, however the maximum peak overpressure is in good agreement. Therefore, the peak overpressure on the structure at dedicated locations is able to appraise in AUTODYN.

**Table 1** Comparison of peak pressure with different grid arrangement

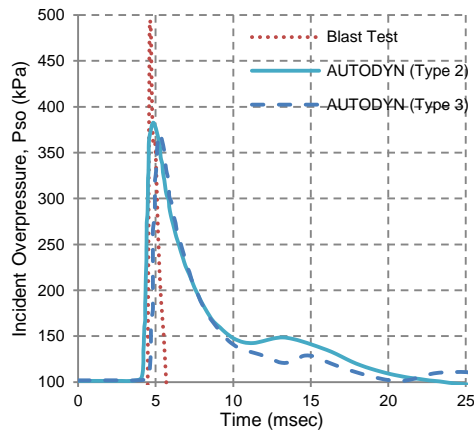
Grid arrangement (I,J,K)axis	Overpressure parameters		Remarks
	Peak pressure (MPa)	Time of arrival (msec)	
(31,31,30)	0.31	5.34	Pressure back to ambient at 30 msec above
(21,23,58)	0.36	5.00	Pressure didn't back to ambient pressure
(18,22,72)	0.38	4.86	Pressure back to ambient at 25 msec

Figure 10 shows the gauges result from the numerical simulation, it can be noticed for the gauge at 18 ft. away, the peak incident overpressure is identical with 0.38 MPa at 4.86 msec and 0.37 MPa at 5.30 msec for air domain Type 2 and air domain Type 3 respectively. It is revealed, with the extension of the air domain as shown in Figure 8 and 9 with the grid on I,J,K (50,50,200) directions respectively, the overpressure positive duration is reduced from 23 msec to 20 msec. In Figure 11, the calculation of incident overpressure at 18 ft. away from UFC-3-340-2 is significant at the lowest pressure compared to the actual blast test. Although the computed incident overpressure data from A.T Blast is close to blast test data, the time arrival is slightly higher. It can be noticed that the incident overpressure parameter for numerical analysis Type 2 and Type 3 are in the range between the blast test, A.T Blast and UFC 3-340-2 parameters. The slight difference with the actual blast test maybe due to outflow boundary is allowed at ground surface. In the real blast situation, if the ground is a perfectly rigid surface, approximately half of the explosion energy would be reflected from the ground effectively doubling the blast wave intensity. For the ground, some energy is lost about 20% in producing ground shock and forming a crater [11].

Figure 12(a) shows the comparison blast overpressure at 4 ft. away from explosive center on the free side. As can be seen, the calculated incident overpressure for UFC 3-340-2 is significantly higher than the numerical analysis for free field explosion (Type 1). However, with the consideration of structure in air volume, the incident overpressure for numerical analysis Type 2 and Type 3 is slightly higher. But for the time arrival to reach to the peak overpressure for UFC 3-340-2, Type 2 and Type 3 is instaneously faster compared to Type 1. This can be concluded with the obstruction nearby the gauges, it shows the overpressure is higher and faster than the gauge at the same distance on the free side in the free-air explosion (Type 1). It is proved that the blast wave reflection on the structure side magnifying the overpressure on the free side. Meanwhile, Figure 12(b) shows the overpressure parameters at 4ft. away from explosive center on the structure side. An analysis of UFC 3-340-2 and ConWep reveals that the overpressure is about 4-6 times higher than numerical analysis. A substantial difference might be due to the reflected overpressure curve in the plot which is based on the reflection off an infinitely large rigid wall to the shock wave. While the wall size of the experimental is significantly smaller compared to the wall tested by Department of Defense, USA [8]. In addition, the numerical simulation of coupled airblast-structure analysis estimates the reduced reflected overpressure computationally. The clearing effect can lead to further reduction of the reflected pressure [20].

The three gauges are located at the height of 538 mm (Bottom), 1270 mm (Middle height) and 1798mm (Top edge) from the ground level on the wall surface in the numerical analysis, it reveals that overpressure at the bottom is the highest. Figure 13 shows the overpressure-time history for each gauges. The highest overpressure for Type 2 is 6.88 MPa at 0.32 msec, while for Type 3 is 12.90 MPa at 0.20 msec which is almost identical in positive duration time. From the experiment conducted by Yan et. al [18], it is found that the peak strain at the bottom of the front face is larger than in the middle height. Generally for the wave propagation, when the shock wave is induced from the explosion, pressure wave will reach the front face first, where a reflection wave will be produced. Besides the reflection wave, part of the wave will also transmit trough the wall, arriving at the back face, another relection wave and transmission wave will be produced. At the bottom of the wall, in addition of the direct wave and its reflection, the reflection wave of the wave on the base surface will have vital impact on the bottom part of the wall. The combination of these waves at the bottom was

caused larger deformation at the bottom part of the wall than that in the middle height, where large cracks were observed at the wall-base corner [18,20]. Therefore, it can be said, as the more surfaces obstruct the wave propagation, the more reflection occurs and magnifies the overpressure. Hence, the highest overpressure at the bottom gauge of numerical simulation is proved. With respect to larger air volume, it reveals that the blast overpressure at the bottom part of Type 2 is almost 3 times higher than Type 3. This might happens due to the reflection wave propagation of Type 3 is more condensed compared to Type 2. In Type 2, the outflow boundary is near to left side of the wall, but in Type 3 the outflow boundary is located more than 18 ft. away from the wall.



**Figure 10.** Blast overpressure-time history

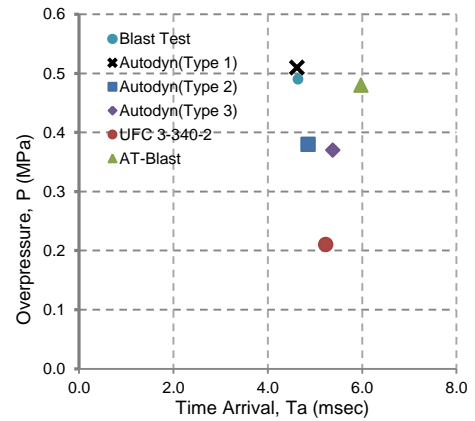


**Figure 11.** Peak pressure at 18 ft. away

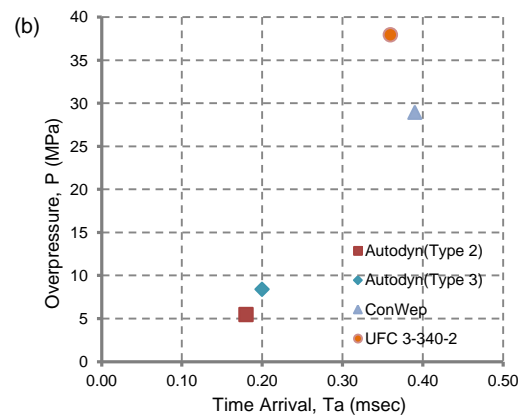
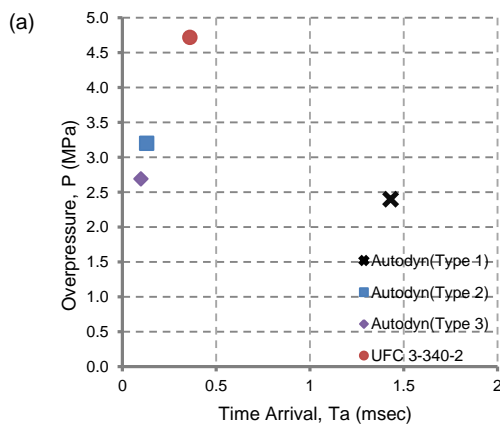


**Figure 12.** Peak Overpressure(a) 4 ft. away on free side (b) 4 ft. away on structure side (wall surface)

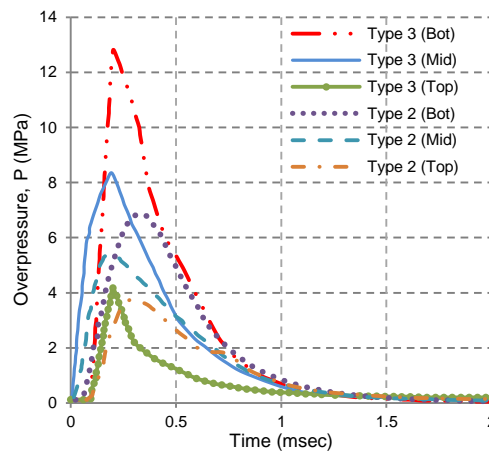


**Figure 13.** Overpressure-time history on wall surface

## 7. Conclusion

In this paper, some of the fundamental studies of blast and its parameters have been outlined. Numerical simulation has been performed to simulate the blast propagation and overpressure study on the cantilevered RC wall and surrounding area. A comparison is made between empirical, numerical and experimental for the same location. According to the result presented in the paper, it indicates that the use of empirical method is not accurate in evaluating overpressure at 18 ft. away from centre of the explosion. However, the numerical result shows that the present simulation result providing more reliable result. Therefore, the overpressure on the wall surface can be predicted. It is also found that the blast overpressure at the bottom part on the wall surface receiving the highest overpressure, and the larger air volume in the simulation will increase the overpressure. On the contrary, the blast pressure distribution on the wall surface for the empirical study is identical either at the top or bottom surface. This is because the capability of the numerical analysis to couple different solver together in space and time, where the consideration of complicity of the flow process involves in forming blast wave, obstruction and its interaction. It is vital to assign proper element distribution and outflow boundary for air volume in the numerical method for obtaining agreeable results close to the experimental parameters.

## References

- [1] Brode H L 1955 Numerical Solution of Spherical Waves *J. Appl. Physic*, vol. 26, pp. 766–775
- [2] Newmark N M and Hansen R J 1961 *Design of blast resistant structure, Shock and Vibration Handbook* (New Jersey, USA: McGraw-Hill) More references
- [3] Henrych J 1979 *The dynamic of explosion and its use* (Elsevier Scientific Publishing Company)
- [4] Kingery C N and Bulmash G 1984 *Air Blast Parameters from TNT Spherical Air Burst and Hemispherical Surface Burst* (Aberdeen:US Army Research Center-Ballistic Laboratory)
- [5] Mills C A 1987 The design of concrete structure to resist explosion and weapon effects in *Proc. 1<sup>st</sup> Int. Conf. on Concrete for Hazard Protections* p 61–73.
- [6] Smith P D and Hetherington J G 1994 *Blast and ballistic loading of structures* (Butterworth-Heinemann)
- [7] DOD 2002 *Unified facilities criteria (UFC 3-340-01) - Design and analysis of hardened structures to conventional weapons effects* (Department of Defense, United States of America)
- [8] DOD 2008 *Unified facilities criteria (UFC 3-340-02) - Structures to resist the effects of accidental* (Department of Defense, United States of America)
- [9] ANSYS 2011 *User's manual, Release 14* (Canonsburg, PA: ANSYS Inc)
- [10] Ngo T, Mendis P, Gupta A and Ramsay J 2007 Blast Loading and Blast Effects on Structures – An Overview *Electronic J. Struct. Eng Special Issue: Loading on Structures* p 76–91.

- [11] Remennikov A 2007 The state of the art of explosive loads characterisation (Wollongong Uni)
- [12] Uddin N 2010 *Blast protection of civil infrastructures and vehicles using composite, part 1: blast threats and blast loading* (Cambridge: Woodhead Publishing Ltd.)
- [13] May G C and Smith P D 1995 *Blast effects on building* (London: Thomas Telford)
- [14] ASCE 1999 *Structural design for physical security-state of the practice* (American Society of Civil Engineers)
- [15] Johansson M and Laine L 2007 *The capacity of buildings to resist severe dynamic loading, part 1: blast wave loading* (Karlstad, Sweden)
- [16] Baker W E 1973 *Explosion in Air* (University of Texas Press)
- [17] Lam N Mendis P and Ngo T 2004 Response Spectrum Solutions for Blast Loading *Electron. J. Struct. Eng. vol. 4* p 28–44.
- [18] Yan D, Chen G, Baird J, Yin H and Koenigstein M 2011 Blast Test of Full-Size Wall Barriers Reinforced with Enamel-Coated Steel Rebar *Struct. Congress ASCE* p 1538–1551.
- [19] Chen G, Brow R K, Jason B, Signo R, Yan D, Koenigstein M and Philip G 2008 *Blast protection of critical infrastructure by used of concrete barriers reinforced with enamel coated steel rebar and fibers* (Missouri:Leonard Wood Institute)
- [20] Kambouchev N, Noels L and Radovitzky R 2007 Numerical simulation of the fluid–structure interaction between air blast waves and free-standing plates *Comput. Struct. vol. 85* p 923–931.